The Disulfide Bridge in the Head Domain of *Rhodobacter sphaeroides* Cytochrome c_1 Is Needed To Maintain Its Structural Integrity†

Maria Elberry, Linda Yu, and Chang-An Yu*

Department of Biochemistry and Molecular Biology, Oklahoma State University, Stillwater, Oklahoma 74078

Received November 1, 2005; Revised Manuscript Received December 12, 2005

ABSTRACT: Cytochrome c_1 of *Rhodobacter sphaeroides* ubiquinol-cytochrome *c* oxidoreductase contains several insertions and deletions that distinguish it from the complex of other higher organisms. Additionally, this bacterial cytochrome c_1 contains two nonconserved cysteines, C145 and C169, with the latter included in the second long insertion located upstream of the sixth heme ligand, M185. The orientation of the insertions and the state of these non-heme binding cysteines remain unknown. Mutating one or both cysteines is found to have comparable effects on the functionality of the cytochrome bc_1 complex. Mutants show an electron transfer activity decreased to a rate that is still high enough to support delayed photosynthetic growth. The mutated cytochrome c_1 has a decreased E_m without any alteration in the heme ligation environment since none of the mutants binds carbon monoxide. The low E_m is believed to be caused by a structural modification in the head domain of cytochrome c_1. Analysis of the mutants reveals that the two cysteines form a disulfide bridge. Cleavage of cytochrome c_1 between the two cysteines followed by gel electrophoresis shows two fragments only under reducing conditions, confirming the existence of a disulfide bridge. The disulfide bridge is essential in maintaining the structural integrity of cytochrome c_1 and thus the functionality of the cytochrome bc_1 complex.

The cytochrome bc_1 complex[1] is a vital component of the electron transfer pathway of mitochondria and many respiratory and photosynthetic bacteria (*1*). It catalyzes the electron transfer from quinol to a *c*-type cytochrome with generation of a proton gradient and membrane potential used for ATP synthesis. All cytochrome bc_1 complexes contain three redox subunits housing a total of four redox centers: cytochrome *b*, which houses two *b*-type hemes (b_L or b_{566} and b_H or b_{562}), cytochrome c_1 which houses a *c*-type heme (c_1), and the Rieske iron−sulfur protein, which houses a high-potential [2Fe-2S] cluster (*1*, *2*). A varying number of additional supernumerary subunits (one to eight) are present in some types of cytochrome bc_1 complex. It is generally accepted that the cytochrome bc_1 complex operates through the Q cycle mechanism, first proposed by Mitchell (*3*). A complete Q cycle results in the oxidation of two quinol molecules and the reduction of two cyt *c* molecules through cyt c_1 and one quinone molecule through hemes b_L and b_H (*4*).

Structurally, cytochrome c_1 basic folds are similar to that of cyt *c* and other class I cytochromes with some insertions and deletions in different linker peptides between the core helices (*5*). It assembles into an extrinsic hydrophilic domain (head domain) anchored to the membrane through a C-terminal hydrophobic transmembrane α-helix (tail domain). Cyt c_1 provides an ionic docking site for cyt *c*, formed by negatively charged aspartic and glutamic acid residues that interact with positively charged lysine residues on the surface of cyt *c* (*6*−*9*). More recent results indicate that the interface between cyt *c* and *Saccharomyces cerevisiae* cyt c_1 includes charged residues as well as hydrophobic residues (*10*) that are necessary to ensure proper binding of cyt *c* to cyt c_1 to allow direct electron transfer (*11*, *12*). Cyt c_1 is reduced by ISP and oxidized by cyt *c* during the catalysis of the cyt bc_1 complex (*2*, *13*).

Rhodobacter sphaeroides cytochrome c_1 contains a conserved CXXCH heme-binding consensus sequence in the head domain, located 37 residues downstream of the N-terminus that covalently binds the heme group through the two cysteines, Cys36 and Cys39. The fifth axial ligand to the heme iron is His40, and the sixth axial ligand is a conserved methionine located at residue 185, close to the C-terminus. Sequence alignment between bovine and *Rb. sphaeroides* cyt c_1 reveals two fragment insertions in the bacterial cyt c_1. The first 17-amino acid fragment (extra fragment Loop 1) extends from residue Gly109 to Ile125 located downstream of the conserved PDL sequence, and the second 19-amino acid fragment (extra fragment Loop 2) extends from residue Gln161 to Ala179 located upstream of the sixth ligand to the heme, Met185. These insertions are absent in cytochrome c_1 forms of higher organisms, such as bovine and yeast, and some bacterial organisms, such as *Rhodospirillum rubrum* and *Paracoccus denitrificans*, but

† This work was supported by Grant MCB0077650 (to L.Y.) from the National Science Foundation, Grant GM30721 (to C.-A.Y.) from the National Institutes of Health, and the Oklahoma Agricultural Experiment Station (Projects 1819 and 2372), Oklahoma State University.

* To whom correspondence should be addressed. E-mail: cayuq@okstate.edu. Telephone: (405) 744-6612. Fax: (405) 744-7799.

[1] Abbreviations: bc_1 complex, ubiquinol-cytochrome *c* oxidoreductase; b_H, higher-potential cytochrome *b* heme; b_L, lower-potential cytochrome *b* heme; CO, carbon monoxide; cyt, cytochrome; DSC, differential scanning calorimetry; EDTA, ethylenediaminetetraacetic acid; E_m, midpoint potential; HRP, horseradish peroxidase; ISP, Rieske iron−sulfur protein; Km, kanamycin; LB, Luria broth; LM, *N*-dodecyl β-D-maltoside; β-ME, β-mercaptoethanol; Ni−NTA, nickel−nitrilotriacetic acid; PAGE, polyacrylamide gel electrophoresis; Q, ubiquinone; $Q_0C_{10}Br$, 2,3-dimethoxy-5-methyl-6-(10-bromodecyl)-1,4-benzoquinol; SDS, sodium dodecyl sulfate; T_m, melting temperature; TMBZ, 3,3′,5,5′-tetramethylbenzidine dihydrochloride; [2Fe-2S], Rieske iron−sulfur center.

10.1021/bi0522246 CCC: $33.50
Published on Web 03/25/2006

are present in *Rhodobacter capsulatus* and *Rb. sphaeroides*. The second extra fragment includes a cysteine at residue 169 that aligns with Cys167 of *Rb. capsulatus*. Another cysteine residue is located at position 145 in *Rb. sphaeroides* that aligns with Cys144 in *Rb. capsulatus*. Because the two cysteines are absent in the cyt c_1 sequence of higher organisms, such as bovine, chicken, and yeast, the crystal structure of which was determined (*10*, *14*−*17*), no structural data can assert the orientation and state of the cysteine residues in the native *Rb. sphaeroides* bc_1 complex.

Recently, Ozyczka et al. (*18*) reported that the two cysteines in *Rb. capsulatus* cyt c_1 form a disulfide bridge. When the bridge is disrupted, a second site suppression mutation of Ala181 to a β-branched amino acid (Thr or Val) spontaneously occurs and restores the functionality of the cytochrome bc_1 complex. This mutation was found to be located two residues away (βXM) from the sixth axial ligand to the heme, Met183. The presence of either the disulfide bond or the βXM amino acid was found to be sufficient to maintain an active cytochrome bc_1 complex. When cysteines were mutated to alanine and a β-branched amino acid was inserted at position βXM, the redox potential of *Rb. capsulatus* cyt c_1 was lowered from 320 to 227 mV, which is comparable to that of wild-type *Rb. sphaeroides* cyt c_1. This would suggest that cyt c_1 of *Rb. sphaeroides* which has properties comparable to those of the mutant, with a β-branched amino acid (Ile183) at position βXM and a redox potential of 235 mV, does not have a disulfide bond). The presence of a disulfide bond in *Rb. capsulatus* cyt c_1 was confirmed by determining the crystal structure of the *Rb. capsulatus* cytochrome bc_1 complex at 3.8 Å (*19*).

Herein, we investigate the state of the cysteines in *Rb. sphaeroides* cyt c_1 using genetic and biochemical techniques. The photosynthetic growth behavior, cyt bc_1 complex activity, and stability and redox potential of cyt c_1 in a purified complex from wild-type and mutant strains were determined and examined. Factor Xa catalysis was performed and analyzed by SDS−PAGE and Western blotting. All results reveal that the two non-heme binding cysteines are connected through a disulfide bridge. We believe that when the bridge is disrupted, the second extra fragment loop (Gln161−Ala179) which includes one of the cysteines is released, resulting in the fluctuation of the loop. This structural alteration results in a change in the functionality of cyt c_1 and the stability of the cyt bc_1 complex.

MATERIALS AND METHODS

Cytochrome *c* (from horse heart, type III) and TMBZ (3,3′,5,5′-tetramethylbenzidine dihydrochloride) were purchased from Sigma. *N*-Dodecyl β-D-maltoside (LM) and *N*-octyl β-D-glucoside (OG) were from Anatrace. Ni−NTA gel and the Qiaprep Spin Miniprep Kit were from Qiagen. 2,3-Dimethoxy-5-methyl-6-(10-bromodecyl)-1,4-benzoquinol ($Q_0C_{10}BrH_2$) was prepared in our laboratory as previously reported (*20*). Bovine heart cyt c_1 was purified according to the previously published method (*21*).

Growth of Bacteria. Escherichia coli cells were grown at 37 °C in LB medium. *Rb. sphaeroides* BC17 cells bearing the pRKD418-*fbc*FBC$_{6H}$Q (*22*) plasmid were grown photosynthetically at 30 °C in an enriched sistrom medium containing 5 mM glutamate and 0.2% casamino acids. Photosynthetic growth conditions for *Rb. sphaeroides* were essentially as described previously (*23*). Antibiotics were added to the following concentrations: 125 μg/mL ampicillin, 20 μg/mL kanamycin sulfate, 25 μg/mL trimethoprim, and 10 μg/mL tetracycline for *E. coli* or 1 μg/mL tetracycline for *Rb. sphaeroides*.

Generation of Rb. sphaeroides-Expressing Mutants of the bc_1 Complex. Mutations were constructed by site-directed mutagenesis using the QuickChange system from Stratagene. The double-stranded pGEM7Zf(+)-C$_{6H}$Q was used as a template. pGEMC$_{6H}$Q was constructed by ligating the *Xba*I−*Hin*dIII fragment of pRKD418-*fbc*FBC$_{6H}$Q (*22*) into the *Xba*I−*Hin*dIII-digested pGEM7Zf(+). The following primers were used to introduce single mutations into cyt c_1: C145A−F, 5′CGGAAGAGCCGCCGAAAGCCGCCGAAGGCCATGAGCC3′; C145A−R, 5′GGCTCATGGCCTTCGGCGGCTTTCGGCGGCTCTTCCG3′; C169A−F, 5′CGGTCCCCGACACCGCCAAGGACGCGAACGGCG3′; C169A−R, 5′CGCCGTTCGCGTCCTTGGCGGTGTCGGGGACCG3′; C145S−F, 5′GAGCCGCCGAAAAGCGCCGAAGCC3′; C145S−R, 5′GGCCTTCGGCGCTTTTCGGCGGCTC3′ C169S−F, 5′CGGTCCCCGACACCAGCAAGGACGCGAAC3′; and C169S−R, 5′GTTCGCGTCCTTGCTGGTGTCGGGGACCG3′.

A template with a C145S/C169S double mutation was constructed using pGEM7fZ(+)-C$_{6H}$Q with a single mutation at C145S as a template and C169S primers. A similar method was used to construct C145A/C169A.

The following primers were used to introduce a Factor Xa cleavage site: P151I/F154R−F, 5′GCCGAAGGCCATGAGATCGACGGCAGGTACTACAACCGCGCCTTC3′ P151I/F154R−R, 5′GAAGGCGCGGTTGTAGTACCTGCCGTCGATCTCATGGCCTTCGGC3′.

The presence of mutations on cyt c_1 was confirmed by DNA sequencing which was carried out at the Recombinant DNA/Protein Core Facility at Oklahoma State University. Plasmid bearing successful cyt c_1 mutations (C*) was digested with *Xba*I and *Hin*dIII, and the generated C*$_{6H}$Q-bearing fragment was purified and ligated to the pRKD418-*fbc*FB vector, generated from the digestion of the pRKD418-*fbc*FBC$_{6H,Km}$Q plasmid with *Xba*I and *Hin*dIII. The generated pRKD*fbc*FBC*$_{6H}$Q plasmid was chemically transformed into *E. coli* S17 cells. A plate mating procedure (*22*) was then used to mobilize the plasmid from *E. coli* S17 into *Rb. sphaeroides* BC17.

Purification of the Cyt bc_1 Complex from Rb. sphaeroides. Chromatophore membranes were prepared as described previously (*24*) and stored at −80 °C in the presence of 20% glycerol until they were used. Frozen chromatophores were used to prepare the cyt bc_1 complex and stored at −80 °C in the presence of 10% glycerol as decribed by Tian et al. (*24*)

Protein concentrations were determined on the basis of the absorbance at 280 nm using a converting factor of 1 $OD_{280} = 0.56\ M^{-1}\ cm^{-1}$. Cyt *b* (*25*) and cyt c_1 (*26*) concentrations were determined spectrophotometrically as published previously.

Activity Assay of the Purified bc_1 Complex. To assay the activity of the cyt bc_1 complex in a chromatophore membranes or purified proteins, the preparations were diluted to a final cyt *b* concentration of 3 μM with 50 mM Tris-HCl (pH 8.0) containing 200 mM NaCl and 0.01% LM. Aliquots of 2, 4, or 6 μL of the diluted sample was added to 1 mL of assay mixture containing 0.3 mM EDTA, and 100 μM cyt *c*

in 100 mM Na^+/K^+ phosphate buffer (pH 7.4). The assays were started by addition of 25 μM $Q_0C_{10}BrH_2$. Activity was determined by assessing the reduction of cyt *c*, which is monitored by the increase in absorbance at 550 nm in a Shimadzu UV2102 PC spectrophotometer at 23 °C, using a millimolar extinction coefficient of 18.5. For calculation purposes, the nonenzymatic oxidation of $Q_0C_{10}BrH_2$ in the absence of enzyme under these conditions was subtracted.

Gel Electrophoresis and Western Blot Preparation and TMBZ Heme Staining. Sodium dodecyl sulfate−polyacrylamide gel electrophoresis (SDS−PAGE) was performed according to the method of Laemmli (*28*) using a Bio-Rad Mini Protean dual-slab vertical cell. Samples were digested with 10 mM Tris-HCl buffer (pH 6.8) containing 1% SDS and 3% glycerol in the presence or absence of 0.4% β-mercaptoethanol for 15−30 min at 23 °C before being subjected to electrophoresis.

Western blotting was performed with rabbit monoclonal antibodies against cyt c_1 or against the His tag. The polypeptides separated by SDS−PAGE were transferred to a polyvinylidene difluoride membrane for immunoblotting. Protein A conjugated to horseradish peroxidase (HRP) was used as second antibody. Color development was carried out using a HRP color development solution.

For TMBZ heme staining, 35 mL of 0.25 M sodium acetate (pH 5.0) was mixed with 15 mL of a freshly prepared solution of 6.3 mM TMBZ and added to the blotted membrane. The membrane was incubated with shaking for 45 min followed by the addition of 1.1 mL of 30% hydrogen peroxide. Color development was observed within 5−15 min.

Cleavage of Heme from Horse Heart Cytochrome c. Apocytochrome *c* was prepared using the silver sulfate method (*27*) with some modifications. Specifically, a mixture of 17 mg of silver sulfate in 1.0 mL of water and 0.1 mL of acetic acid was added to a solution of 6 mg of cyt *c* dissolved in water. The mixture was incubated at 37 °C for 4.5 h and then centrifuged to remove any precipitation. The treated sample was confirmed to be heme-free cyt *c* when the band was observed on SDS−PAGE with Coomassie blue staining but cannot be detected by TMBZ heme staining.

Carbon Monoxide Binding Experiment. A carbon monoxide (CO) binding experiment was performed at room temperature. Fully oxidized purified protein (2.5 μM), dissolved in 100 mM Tris-HCl (pH 8.0) containing 100 mM NaCl, was first reduced with dithionite, and the spectrum was recorded (specR), followed by a short bubbling with carbon monoxide, after which spectra were also recorded (specR+CO). Carbon monoxide binding was analyzed on the basis of specCO which was calculated from specR+CO minus specR spectra. No spectral change is expected if no binding of CO takes place.

Differential scanning calorimetry was performed using N-DSCII. Purified protein (0.55 mL of 15 μM cyt bc_1 complex) was first degassed at room temperature for 10 min. Thermoscans from 10 to 90 °C at rates of 1 and 2 °C/min were performed during the heating and cooling scans, respectively. Three scans were recorded (heating, cooling, and heating) using the third scan as a baseline for the first scan. CpCalc was used to calculate T_m values of purified proteins.

Determination of the Redox Potential of Cytochrome c_1 in the Wild-Type and Mutant bc_1 Complex. The potentiometric titrations of cyt c_1 were essentially done according to the previously published method (*29*, *30*) using the following redox mediators (final concentrations): diaminodurol (70 μM), duroquinone (50 μM), pyocyanine (25 μM), anthroquinone-2-sulfonic acid (25 μM), Indigo carmine (25 μM), 1,2-naphthoquinone (25 μM), 1,4-benzoquinone (20 μM), phenazine ethosulfate (20 μM), and phenazine methosulfate (20 μM). Reductive potentiometric titrations were carried out using dithionite to reduce the ferricyanide-oxidized sample, and ferricyanide was used for oxidative titration of the dithionite-reduced sample. All titrations were performed at room temperature using a sealed anaerobic cuvette constantly flushed with argon. The midpoint potential of cyt c_1 was calculated by fitting the redox titration data obtained to the Nernst equation when $n = 1$.

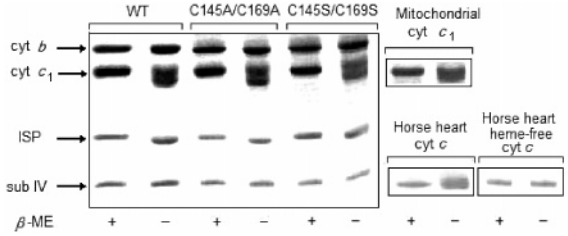

FIGURE 1: SDS−PAGE analysis of the cyt bc_1 complexes isolated from the wild type and cysteine mutants and of bovine heart mitochondrial cyt c_1 and horse heart cyt *c*. Samples of protein (75 pmol) were incubated under reducing (with β-ME) or nonreducing conditions (without β-ME) at room temperature for 30 min.

Factor Xa Proteolysis. The experiment was done on the basis of a previously reported technique (*18*) with some minor modifications. The digestion was done using 150 nmol of purified cyt bc_1 complex in 50 mM Tris-HCl (pH 8.0) containing 100 mM NaCl and 0.01% SDS. The sample was incubated at 50 °C for 10 min. Factor Xa was then added, to a final concentration of 1% of total protein content, and the samples with the enzyme were incubated at room temperature for 16 h. Afterward, loading dye was added, and the sample was incubated at 23 °C for 15 min before being subjected to SDS−PAGE.

RESULTS AND DISCUSSION

Sensitivity of Rb. sphaeroides Cytochrome c_1 to a Reducing Agent in SDS Gel Electrophoresis. SDS gel electrophoresis of *Rb. sphaeroides* cyt c_1 shows sensitivity to a reducing agent, unlike the other three subunits, cytochrome *b*, ISP, and subunit IX (*31*). Under reducing conditions, the cyt c_1 band exists as a sharp band, whereas under nonreducing conditions, it exists as a smeared band. It was suggested that sensitivity to a reducing agent is associated with the presence of a disulfide bridge in the head domain of cyt c_1 between the two non-heme binding cysteines (*31*, *32*), but results presented herein show that in the absence of a potential disulfide bond, cyt c_1 still exists as a smeared band under nonreducing conditions. Both non-heme binding cysteines, C145 and C169, were mutually mutated to alanine and serine to prevent the formation of a disulfide bridge. Cytochrome bc_1 complexes purified from these mutants were subjected to SDS−PAGE under reducing and nonreducing conditions. In each of the double mutants of cysteines to alanines (C145A/C169A) and cysteines to serines (C145S/C169S), cyt c_1 exists as a sharp band under reducing conditions and as a smeared band under nonreducing conditions (Figure 1). These results contradict the previously suggested hypothesis

Table 1: Summary of Wild-Type and Mutant Characteristics[a]

strain	Ps. growth	enzymatic activity [μmol of cyt *c* reduced min^{-1} (nmol of cyt *b*)$^{-1}$]	T_m (°C)	% cyt c_1 reduced by Asc	cytochrome c_1 heme	
					E_m (mV)	CO binding
wild type	+++	2.5	45.2	100	235	−
C145A	++	2.0	42.4	40	64	−
C169A	++	2.0	42.2	40	62	−
C145A/C169A	++	2.0	41.9	40	59	−
C145S	+	1.5	41.1	25	48	−
C169S	+	1.5	41.4	25	49	−
C145S/C169S	+	1.5	41.8	25	51	−
P151I/F154R	+++	2.5	44.9	100	210	−

[a] In the Ps. growth column, ++ and + refer to a photosynthetic growth rate delayed by 24 and 36 h, respectively, as compared to the wild-type photosynthetic growth rate (+++). Methods used to calculate enzymatic activity, T_m, E_m, and CO binding are described in Materials and Methods. The data are mean values from three experiments.

and confirm that the sensitivity of cyt c_1 to a reducing agent is not related to the presence of a disulfide bond.

To examine whether such behavior is observed with only *Rb. sphaeroides* cyt c_1 or with other *c*-type cytochromes as well, horse heart cyt *c* and bovine heart mitochondrial cyt c_1 were subjected to SDS−PAGE under reducing and nonreducing conditions (Figure 1). Results show that both *c*-type cytochromes are also sensitive to the presence of a reducing agent. Both *c*-type cytochromes exist as a sharp band and as a smeared band in the presence and absence of β-mercaptoethanol, respectively. However, *Rb. capsulatus* cyt c_1, which contains a disulfide bridge between the nonheme binding cysteines, exhibits no such sensitivity and appears as a sharp band under reducing and nonreducing conditions (*18*). The reason *Rb. capsulatus* cyt c_1 does not exist as a smeared band under nonreducing conditions is most likely due to the small amount of sample used, because when a small amount of horse cyt *c* and larger wells are used, a sharper band is observed under nonreducing conditions. Since neither horse heart cyt *c* (*33*) nor bovine heart mitochondrial cyt c_1 (*34*, *35*) has a disulfide bond, we believe that the sensitivity of cyt c_1 to the presence or absence of a reducing agent is not associated with the presence of disulfide bond(s).

The major difference between *c*-type cytochrome and the other protein is the presence of a covalently bound heme. To examine whether the observed electrophoretic behavior is associated with the presence of the linked heme, the heme was cleaved from horse heart cytochrome *c* and the generated apocytochrome *c* was subjected to SDS−PAGE and TMBZ heme staining. The cyt *c* band can be visualized via SDS−PAGE (Figure 1) but cannot be stained by TMBZ which confirms that the heme is lost. Apocytochrome *c* exhibits similar behavior under reducing and nonreducing conditions which suggests that the sensitivity of *c*-type cytochromes to the presence of a reducing agent is associated with its covalently linked heme rather than the presence of a disulfide bond.

Analysis of Cysteine Mutants in Cytochrome c_1. The nonheme binding cysteine residues in cyt c_1, C145 and C169, were mutated to alanine individually to generate the mutants C145A and C169A and mutually to generate the double mutant C145A/C169A. Characteristics of these mutants, summarized in Table 1, reveal that mutating cysteine to alanine does not severely affect the cyt bc_1 activity. Mutants can still grow photosynthetically but with a delay of 24 h,

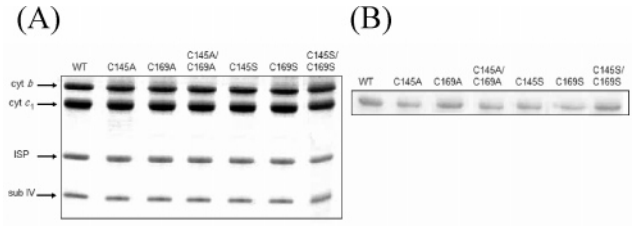

FIGURE 2: (A) SDS−PAGE and (B) TMBZ heme staining analysis of the cyt bc_1 complexes isolated from the wild type and cysteine mutants. Samples of protein (70 pmol) were incubated in the presence of β-mercaptoethanol as a reducing agent at room temperature for 15 min.

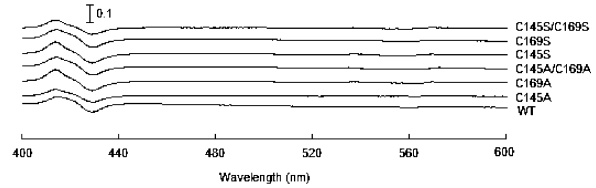

FIGURE 3: Carbon monoxide optical difference spectra of the cyt bc_1 complexes isolated from wild type and each of the single and double alanine and serine mutants. Carbon monoxide binding was analyzed on the basis of the calculation from specR+CO minus specR spectra as described in Materials and Methods.

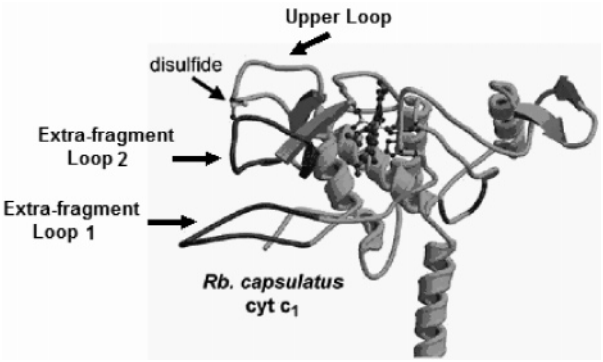

FIGURE 4: Structure of *Rb. capsulatus* cyt c_1 as reported by Berry et al. (*26*) used as a model to predict the structural effect of cysteine mutations in *Rb. sphaeroides* cyt c_1. The disulfide bond between the two cysteines is labeled "disulfide". The two long extra fragment loops present in both *Rb. capsulatus* and *Rb. sphaeroides* cyt c_1 are labeled extra fragment loop 1 and loop 2 in this figure. The top loop contains the first cysteine (C145 in *Rb. sphaeroides* and C144 in *Rb. capsulatus*).

and ~80% of wild-type activity is retained in each of the single and double mutants. These results suggest that the cysteines might be connected through a disulfide bridge since

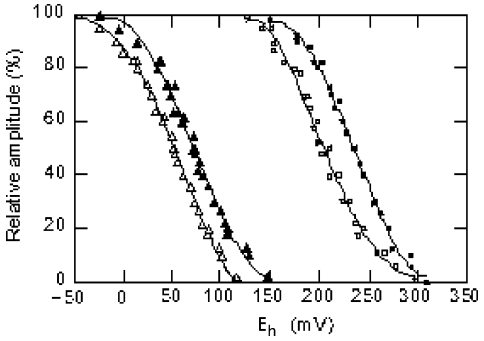

FIGURE 5: Potentiometric titration of cytochrome c_1 in purified cytochrome bc_1 complexes from the wild type, P151I/F154R, and one of each of the mutants of cysteine to alanine and serine: (■) wild type (E_m = 235 mV), (□) P151I/F154R (E_m = 210 mV), (▲) C145A (E_m = 64 mV), and (△) C145S (E_m = 48 mV). The E_m values for C169A, C145A/C169A, C169S, and C145S/C169S mutants are listed in Table 1. Oxidative and reductive titrations were performed as described in Materials and Methods. The data were fit to the Nernst equation when n = 1.

mutating one or both cysteines disrupts the disulfide bridge and has the same effect on mutant growth and mutant bc_1 complex activity. One way to examine the structural importance of potential free cysteines is to mutate each cysteine or both cysteines to serine, a structurally similar amino acid, generating the single mutants C145S and C169S and the double mutant C145S/C169S. Serine mutants also grow photosynthetically but with a delay of 36 h as compared to wild type, and only 60% of wild-type activity is retained, which is lower than the alanine mutant activity. These results also imply that the cysteines are linked with a disulfide bridge in the native protein, and disruption of the bridge and insertion of two hydroxyl groups result in an additional defect which results in lower protein activity. All purified mutant complexes were subjected to SDS−PAGE, and no difference was observed compared to the wild type; all mutant complexes contain all four subunits with comparable intensity with the heme group covalently bound to cyt c_1, detected by TMBZ heme staining (Figure 2).

Differential scanning calorimetry was used to check the stability of the mutant proteins. The melting temperatures (T_m) of mutant cytochrome bc_1 complexes were found to be 2.8−4.1 °C lower than that of the wild-type bc_1 complex (Table 1), which suggests that the disulfide bridge is required to maintain protein stability. Lower activity and stability of the bc_1 complex might be associated with a change in the heme environment of cyt c_1 caused by the disruption of the disulfide bond. To examine if any of the heme ligands of cyt c_1 was altered by eliminating the disulfide bridge, we tested the ability of the mutant proteins to bind carbon monoxide. The difference dithionite reduced + CO minus dithionite reduced spectra of the mutated bc_1 complex were recorded and were found to be comparable to the wild-type profile (Figure 3), which indicates that the ligands of heme c_1 are not affected by the disruption of the disulfide bond.

Since *Rb. sphaeroides* and *Rb. capsulatus* cyt c_1 are closely related and structurally comparable due to the high percentage of identity between the sequences, determining the structure of the *Rb. capsulatus* cyt bc_1 complex (*19*) and of the cyt c_1 head domain specifically (Figure 4) allowed us to predict and visualize the possible structural alterations upon disruption of the disulfide bridge. We believe that disrupting the disulfide bridge, which fixes the extra fragment loop 2 close to the upper loop, results in the release of the extra fragment loop 2, fluctuation of which between the upper loop and the lower loop (extra fragment loop 1) affects cyt c_1 functionality, as shown by lower enzyme activity, and cyt bc_1 complex stability, as shown by lower T_m values.

Effect of Cysteine Mutation on the Midpoint Potential of Cytochrome c_1. Mutating the cysteines significantly affects the redox potential of cyt c_1 by lowering it from 230 mV to as low as 59 and 48 mV in each of the alanine and serine mutants, respectively (Figure 5). The decrease in midpoint potential explains why cyt c_1 cannot be fully reduced by ascorbate in any of the cysteine mutants (Table 1). Only ~40 and ~25% of cyt c_1 is reduced by ascorbate in the alanine and serine mutants, respectively. In some proteins, the second extra fragment loop folds close to its native position in the wild-type protein, resulting in a percentage of the population, 40% in alanine mutants and 25% in serine mutants, that can be reduced by ascorbate. In other proteins, the extra fragment

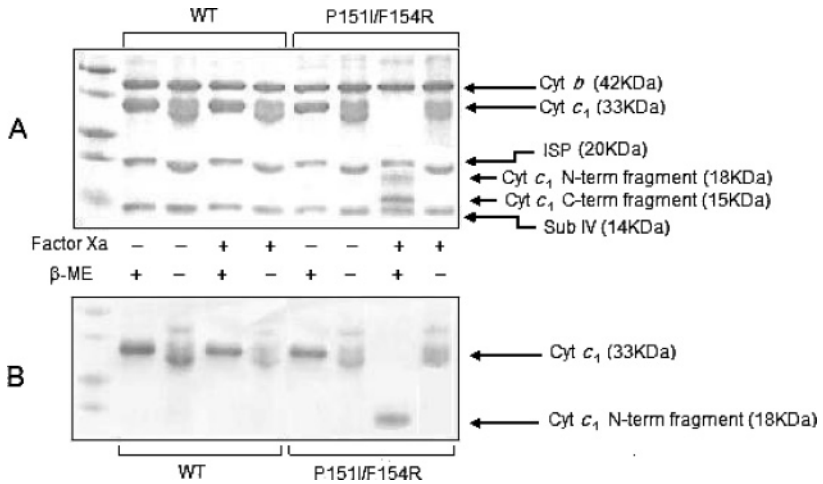

FIGURE 6: SDS−PAGE analysis and TMBZ heme staining of factor Xa cleavage of the cytochrome bc_1 complex of the wild type and P151I/F154R mutant. (A) SDS−PAGE profile of undigested (without factor Xa) and digested (with factor Xa) wild-type and factor Xa cleavable mutant (P151I/F154R) cytochrome bc_1 complex in the presence (with β-ME) and absence (without β-ME) of a reducing agent. Because the factor Xa cleavage site is absent in the wild-type protein, cyt c_1 remains intact when the protein is digested. (B) Heme-containing fragments were stained with TMBZ to further confirm the identity of each fragment. Western blotting against the His tag was performed to confirm the identity of the C-terminal fragment (results not shown).

loop is dislocated farther from its original position, especially upon insertion of a serine residue which causes increased repulsion due its size and polarity, resulting in a decrease in the cyt c_1 midpoint potential below its ability to be reduced by ascorbate. Considering the distance dependence of the electron transfer rate (*36*, *37*), we believe that despite the considerable drop in the cyt c_1 midpoint potential, the short distances between the redox centers of the high-potential chain can still allow rapid electron transfer from ISP through cyt c_1 to cyt *c*, with the assistance of the high potential of cyt *c* (260 mV).

Clearly, the drop in midpoint potential is not caused by the alteration of any of the heme ligands since none of the mutants binds carbon monoxide but is most likely caused by the structural modification caused by releasing the second extra fragment loop affecting the structural integrity around the heme.

Factor Xa Digestion of Cytochrome c_1. If the disulfide bond exists, cleaving cyt c_1 protein (33 kDa) between the two cysteines will generate two polypeptides linked through the disulfide bridge. Therefore, when the product is run on SDS−PAGE under nonreducing conditions, the product will exhibit a profile similar to that of the undigested protein (33 kDa band). However, under reducing conditions where β-mercaptoethanol is used to reduce the disulfide bond, the two peptides will be separated on SDS−PAGE. This approach is valid only if the cleavage site is specific and unique in the protein. Because the amino acid sequence of cyt c_1 does not contain a unique site between the two cysteines, the sequence was screened for the closest match compared to different cleavage enzyme consensus sequences. At positions 151−154, a PDGF sequence was mutated to an IDGR sequence, by generating the P151I and F154R mutations simultaneously to match the factor Xa cleavage consensus sequence (IDGR). P151I/F154R double mutant proteins were purified and characterized, and results are summarized in Table 1. Mutant cells grow photosynthetically at the same rate as the wild-type cells, and the specific activity of purified protein is also comparable to that of the wild type. The midpoint potential of the cyt c_1 double mutant was measured and determined to be 210 mV compared to the wild-type cyt c_1 midpoint potential of 235 mV. Since the P151I/F154R mutant has features similar to those of the wild type, it is believed to have identical structural folding and can be used to test the presence of a disulfide bond in native proteins. Results shown in Figure 6 reveal that the two fragments remain linked under nonreducing conditions and separate into two fragments of 18 and 15 kDa, which represent the N-terminal fragment containing the heme group (Figure 6B) and the C-terminal fragment containing the His tag, respectively. These results confirm that the two non-heme binding cysteines in *Rb. sphaeroides* cyt c_1 form a disulfide bridge.

Disruption of the disulfide bridge seems to result in the release of the second extra fragment loop, fluctuation of which slows the cytochrome bc_1 complex activity and significantly lowers its stability and the redox potential of cytochrome c_1. Unlike *Rb. capsulatus* cytochrome c_1 which necessitates the presence of either the disulfide bond or the βXM motif (*18*) to maintain the integrity of the cytochrome bc_1 complex, *Rb. sphaeroides* cytochrome c_1 requires the presence of a disulfide bridge to modulate the heme potential and the protein stability despite the presence of a branched amino acid (Ile) at the βXM motif.

REFERENCES

1. Trumpower, B. L., and Gennis, R. B. (1994) Energy transduction by cytochrome complexes in mitochondrial and bacterial respiration: The enzymology of coupling electron transfer reactions to transmembrane proton translocation, *Annu. Rev. Biochem. 63*, 675−716.
2. Trumpower, B. L. (1990) The protonmotive Q cycle. Energy transduction by coupling of proton translocation to electron transfer by the cytochrome bc_1 complex, *J. Biol. Chem. 265*, 11409−11412.
3. Mitchell, P. (1976) Possible molecular mechanisms of the protonmotive function of cytochrome systems, *J. Theor. Biol. 62*, 327−367.
4. Berry, E. A., Guergova-Kuras, M., Huang, L. S., and Crofts, A. R. (2000) Structure and function of cytochrome bc complexes, *Annu. Rev. Biochem. 69*, 1005−1075.
5. Zhang, Z. L., Huang, L. S., Shulmeister, V. M., Chi, Y. I., Kim, K. K., Hung, L. W., Crofts, A. R., Berry, E. A., and Kim, S. H. (1998) Electron transfer by domain movement in cytochrome bc_1, *Nature 392*, 677−684.
6. Stonehuerner, J., O'Brien, P., Geren, L., Millet, F., Steidl, J., Yu, L., and Yu, C. A. (1985) Identification of the binding site on cytochrome c_1 for cytochrome *c*, *J. Biol. Chem. 260*, 5392−5398.
7. Nakai, M., Endo, T., Hase, T., Tanaka, Y., Trumpower, B. L., Ishiwatari, H., Asada, A., Bogaki, M., and Matsubara, H. (1993) Acidic regions of cytochrome c_1 are essential for ubiquinol-cytochrome *c* reductase activity in yeast cells lacking the acidic QCR6 protein, *J. Biochem. 114*, 919−925.
8. Guner, S., Willie, A., Millett, F., Caffrey, M. S., Cusanovich, M. A., Robertson, D. E., and Knaff, D. B. (1993) The interaction between cytochrome c_2 and the cytochrome bc_1 complex in the photosynthetic purple bacteria *Rhodobacter capsulatus* and *Rhodopseudomonas viridis*, *Biochemistry 32*, 4793−4800.
9. Tian, H., Sadoski, R., Zhang, L., Yu, C. A., Yu, L., Durham, B., and Millett, F. (2000) Definition of the interaction domain for cytochrome *c* on the cytochrome bc_1 complex. Steady-state and rapid kinetic analysis of electron transfer between cytochrome *c* and *Rhodobacter sphaeroides* cytochrome bc_1 surface mutants, *J. Biol. Chem. 275*, 9587−9595.
10. Lange, C., and Hunte, C. (2002) Crystal structure of the yeast cytochrome bc_1 complex with its bound substrate cytochrome *c*, *Proc. Natl. Acad. Sci. U.S.A. 99*, 2800−2805.
11. Yu, C. A., Yu, L., and King, T. E. (1973) Kinetics of electron transfer between cardiac cytochrome c_1 and *c*, *J. Biol. Chem. 248*, 528−533.
12. Engstrom, G., Rajagukguk, R., Saunders, A. J., Patel, C. N., Rajagukguk, S., Merbitz-Zahradnik, T., Xiao, K., Pielak, G. J., Trumpower, B., Yu, C. A., Yu, L., Durham, B., and Millett, F. (2003) Design of a ruthenium-labeled cytochrome *c* derivative to study electron transfer with the cytochrome bc_1 complex, *Biochemistry 42*, 2816−2824.
13. Xia, D., Kim, H., Yu, C. A., Yu, L., Kachurin, A., Zhang, L., and Deisenhofer, J. (1998) A novel electron transfer mechanism suggested by crystallographic studies of mitochondrial cytochrome bc_1 complex, *Biochem. Cell Biol. 76*, 673−679.
14. Xia, D., Yu, C. A., Kim, H., Xia, J. Z., Kachurin, A. M., Zhang, L., Yu, L., and Deinsenhofer, J. (1997) Crystal structure of the cytochrome bc_1 complex from bovine heart mitochondria, *Science 277*, 60−66.
15. Zhang, Z., Huang, L., Shulmeister, V. M., Chi, Y., Kim, K. K., Hung, L., Crofts, A. R., Berry, E. A., and Kim, S. (1998) Electron transfer by domain movement in cytochrome bc_1, *Nature 392*, 677−684.
16. Iwata, S., Lee, J. W., Okada, K., Lee, J. K., Iwata, M., Rasmussen, B., Link, T. A., Ramaswamy, S., and Jap, B. K. (1998) Complete structure of the 11-subunit bovine mitochondrial cytochrome bc_1 complex, *Science 281*, 64−71.
17. Hunte, C., Koepke, J., Lange, C., Rossmanith, T., and Michel, H. (2000) Structure at 2.3 Å resolution of the cytochrome bc_1 complex from the yeast *Saccharomyces cerevisiae* co-crystallized with an antibody Fv fragment, *Struct. Folding Des. 8*, 669−684.
18. Osyczka, A., Dutton, P. L., Moser, C. C., Darrouzet, E., and Daldal, F. (2001) Controlling the functionality of cytochrome c_1 redox potentials in the *Rhodobacter capsulatus* bc_1 complex through

disulfide anchoring of a loop and a β-branched amino acid near the heme-ligating methionine, *Biochemistry 40*, 14547−14556.
19. Berry, E. A., Huang, L. S., Saechao, L. K., Ning, G. P., Valkova-Valchanova, M., and Daldal, F. (2004) X-ray Structure of *Rhodobacter capsulatus* Cytochrome bc_1: Comparison with its Mitochondrial and Chloroplast Counterparts, *Photosynth. Res. 81*, 251−275.
20. Yu, C. A., and Yu, L. (1982) Synthesis of biologically active ubiquinone derivatives, *Biochemistry 21*, 4096−4101.
21. Yu, C. A., Chiang, Y. L., Yu, L., and King, T. E. (1975) Photoreduction of cytochrome c_1, *J. Biol. Chem. 250*, 6218−6221.
22. Mather, M. W., Yu, L., and Yu, C. A. (1995) The involvement of threonine 160 of cytochrome *b* of *Rhodobacter sphaeroides* cytochrome bc_1 complex in quinone binding and interaction with subunit IV, *J. Biol. Chem. 270*, 28668−28675.
23. Tian, H., Yu, L., Mather, M. W., and Yu, C. A. (1997) The involvement of serine 175 and alanine 185 of cytochrome *b* of *Rhodobacter sphaeroides* cytochrome bc_1 complex in interaction with iron−sulfur protein, *J. Biol. Chem. 272*, 23722−23728.
24. Tian, H., Yu, L., Mather, M. W., and Yu, C. A. (1998) Flexibility of the neck region of the Rieske iron−sulfur protein is functionally important in the cytochrome bc_1 complex, *J. Biol. Chem. 273*, 27953−27959.
25. Berden, J. A., and Slater, E. C. (1970) The reaction of antimycin with a cytochrome *b* preparation active in reconstitution of the respiratory chain, *Biochim. Biophys. Acta 216*, 237−249.
26. Yu, L., Dong, J. H., and Yu, C. A. (1986) Characterization of purified cytochrome c_1 from *Rhodobacter sphaeroides* R-26, *Biochim. Biophys. Acta 852*, 203−211.
27. Fisher, W., Taniushi, H., and Anfinsen, C. (1973) On the role of heme in the formation of the structure of cytochrome *c*, *J. Biol. Chem. 248*, 3188−3195.
28. Laemmli, U. K. (1970) Cleavage of structural proteins during the assembly of the head of bacteriophage T4, *Nature 227*, 680−685.
29. Dutton, P. L. (1978) Redox potentiometry: Determination of midpoint potentials of oxidation−reduction components of biological electron-transfer systems, *Methods Enzymol. 54*, 411−435.
30. Guner, S., Robertson, D. E., Yu, L., Qiu, Z. H., Yu, C. A., and Knaff, D. B. (1991) The *Rhodospirillum rubrum* cytochrome bc_1 complex: Redox properties, inhibitor sensitivity and proton pumping, *Biochim. Biophys. Acta 1058*, 269−279.
31. Xiao, K., Yu, L., and Yu, C. A. (2000) Confirmation of the involvement of protein domain movement during the catalytic cycle of the cytochrome bc_1 complex by the formation of an intersubunit disulfide bond between cytochrome *b* and the iron−sulfur protein, *J. Biol. Chem. 275*, 38597−38604.
32. Konishi, K., Van Doren, S. R., Kramer, D. M., Crofts, A. R., and Gennis, R. B. (1991) Preparation and characterization of the water-soluble heme-binding domain of cytochrome c_1 from the *Rhodobacter sphaeroides* bc_1 complex, *J. Biol. Chem. 266*, 14270−14276.
33. Qi, P. X., Di Stefano, D. L., and Wand, A. J. (1994) Solution structure of horse heart ferrocytochrome *c* determined by high-resolution NMR and restrained simulated annealing, *Biochemistry 33*, 6408−6417.
34. Xia, D., Yu, C. A., Kim, H., Xia, J. Z., Kachurin, A. M., Zhang, L., Yu, L., and Deisenhofer, J. (1997) Crystal structure of the cytochrome bc_1 complex from bovine heart mitochondria, *Science 277*, 60−66.
35. Esser, L., Quinn, B., Li, Y. F., Zhang, M., Elberry, M., Yu, L., Yu, C. A., and Xia, D. (2004) Crystallographic studies of quinol oxidation site inhibitors: A modified classification of inhibitors for the cytochrome bc_1 complex, *J. Mol. Biol. 341*, 281−302.
36. Moser, C. C., Pager, C. C., Farid, R., and Dutton, P. L. (1995) Biological electron transfer, *J. Bioenerg. Biomembr. 27*, 263−274.
37. Crofts, A. R., Barquera, B., Gennis, R. B., Kuras, R., Guegorva-Kuras, M., and Berry, E. A. (1999) Mechanism of ubiquinol oxidation by the bc_1 complex: Different domains of the quinol binding pocket and their role in the mechanism and binding of inhibitors, *Biochemistry 38*, 15807−15826.

BI0522246